Article ID: 1003－6326(2005)06－1420－05

Electrochemical properties of novel calcium stannate anode for lithium ion batteries①

HE Ze-qiang(何则强)[1, 2], XIONG Li-zhi(熊利芝)[1], XIAO Zhuo-bing(肖卓炳)[1], MA Ming-you(麻明友)[1], WU Xian-ming(吴显明)[1], HUANG Ke-long(黄可龙)[2]

(1. College of Chemistry and Chemical Engineering, Jishou University, Jishou 416000, China;
2. School of Chemistry and Chemical Engineering, Central South University, Changsha 410083, China)

Abstract: $CaSnO_3$ with the perovskite structure was prepared by wet-chemical route and the electrochemical properties as anode material for lithium ion batteries were studied. The results show that the uniform nano-crystallites (about 200 nm) of $CaSnO_3$ are obtained and a reversible capacity of 460 mA·h·g^{-1} (0－1.0 V, 0.1 *C*) with good cycling stability is delivered (the capacity loss per cycle is only 0.09%). The observed capacity involved in the first discharge and the reversible capacity during subsequent charge-discharge cycles shows that the electrochemical process in $CaSnO_3$ is similar to other Sn-based oxide materials, namely, an initial structural reduction with Sn metal formation followed by reversible Li-Sn alloy formation. Both the attainable capacity and its retention on charge-discharge cycling are better than the previously reported best-performing bulk Sn-oxide or ATCO materials, which indicates that the perovskite structure and Ca-ion may play a beneficial role.

Key words: lithium ion batteries; $CaSnO_3$; wet chemical route; anode

CLC number: O 612.4 **Document code:** A

1 INTRODUCTION

The reversible alloying and dealloying properties of Sn with Li have gained wide spread interest due to its potentiality to use as anode material in Li-ion batteries[1－8]. The search for Sn-based materials gained momentum after the report of nearly 600 mA·h·g^{-1} reversible capacity observed in amorphous Sn-based composite oxides (ATCO)[1]. By in situ X-ray diffraction, Courtney et al[2, 3] showed that the reversible Li-Sn alloy formation is responsible for the observed reversible capacity in such compounds. Accordingly, the Sn-oxide is irreversibly reduced to metallic Sn and Li_2O during the first discharge followed by the alloying of Sn with Li, which can be written as

$$SnO_y + 2yLi^+ + 2ye \longrightarrow Sn + yLi_2O \quad (y = 1 \text{ or } 2) \quad (1)$$

$$xLi^+ + Sn + xe \longrightarrow Li_xSn \quad (x \leqslant 4.4) \quad (2)$$

Reaction (1) leads to nanostructured Sn domains homogeneously dispersed in the inactive Li_2O matrix. Reaction (2) is reversible and responsible for the capacity. However, the $Li_{4.4}Sn$ alloy formation involves 300% volume change for the Sn matrix causing cracking and crumbling of the electrode resulting in electrical contact isolation and capacity-fading on repeated cycling[3, 4]. Since the reaction (2) takes place in the Li_2O matrix, the accompanied strain can be considerably minimized. However, Courtney et al[2, 3] reported that repeated cycling leads to segregation of Sn metal into larger grains eventually leading to material degradation and capacity loss. Therefore, the strategies adopted to alleviate this drawback of Sn-based electrodes including ATCO are: 1) obtaining the Sn-oxide in the desired morphology (thin film, nanoparticles or in amorphous form) where the effect of volume expansion may be minimized[5－7]; 2) allowing the alloy formation in a matrix of oxides of different crystal systems or intermetallics (active or inactive towards Li) or derivatives of carbon which can considerably prevent the Sn segregation and thereby accommodate the strain on volume expansion on alloying with Li[2－4, 8－10]; 3) suitably selecting the voltage window of the cell operation to minimize secondary reactions[2, 3, 6, 8]. Preparation of thin film electrodes involves complicated experimental procedures and mass manufacture with reproducible and beneficial microstructure and electrochemical properties are difficult to achieve. Therefore, ATCO and Sn-oxides of different

① **Foundation item:** Excellent Youth project(04B016) supported by the Education Office of Hunan Province; Project(20050037700) supported by the Postdoctoral Science Foundation of China; Project(2004107) supported by the Postdoctoral Science Foundation of Central South University, China **Received date:** 2005－02－17; **Accepted date:** 2005－07－12

Correspondence: HE Ze-qiang, PhD; Tel: +86-743-6125318; Fax: +86-743-8563911; E-mail: csuhzq@163.com

crystal systems, which can be obtained in bulk form by simple methods, are of interest[2, 3, 8-10].

Recently, stannates $MSnO_3$ (M = Ca, Sr, Ba) as a component of dielectric materials have received much attention due to their applications as thermally stable capacitors in electronic industries[11]. So far as we know, several authors have studied stannates on their dielectric properties, surface conformations and microstructures[12, 13], but there is few reports on the electrochemical properties of stannates. Here the electrochemical behavior of $CaSnO_3$ with the perovskite structure prepared by wet chemical-route was reported.

2 EXPERIMENTAL

$CaSnO_3$ samples were synthesized by wet-chemical route according to Ref. [14].

The crystalline phase of sample was identified by X-ray diffraction (XRD) (Siemens D500; Cu K_α radiation) and surface morphology was characterized by scanning electron microscopy (SEM) (JEOL JSM-6700F, Field Emission Electron Microscope).

Electrodes for electrochemical characterization were prepared by doctor blade technique with active material ($CaSnO_3$), acetylene black and polyvinylidenefluoride (PVDF) in mass ratio of 70∶20∶10. N-methyl pyrrolidinone (NMP) was used as the solvent and copper foil as current collector. Coin cells (size 2025) with Li foil as counter electrode were fabricated in argon filled glove box. Celgard 2502 membrane was used as separator and 1 mol/L $LiPF_6$ in ethylene carbonate (EC) + diethyl carbonate (DEC) (1∶1 in volume) as the electrolyte. All the electrochemical analyses were carried out with an electrochemical analysis system.

3 RESULTS AND DISCUSSION

Fig. 1 shows the XRD pattern of sample by wet-chemical route.

The XRD pattern shows that formation of phase-pure $CaSnO_3$ with perovskite structure and matches well with the JCPDS file (Card No. 31-312).

The morphology of the sample from the SEM image is shown in Fig. 2. It is clear that the wet-chemical route derived $CaSnO_3$ is composed of uniform crystallites with a narrow particle size distribution of about 200 nm.

Fig. 3 shows the first discharge and charge curves of $CaSnO_3$ anode at a current rate of 0.1 *C*. The discharge profile shows a small plateau at 1.0 V followed by an extended flat potential profile around 0.4 V. Similar to other Sn-based oxides studied earlier[2, 3, 6, 8-10, 15], the process occurring

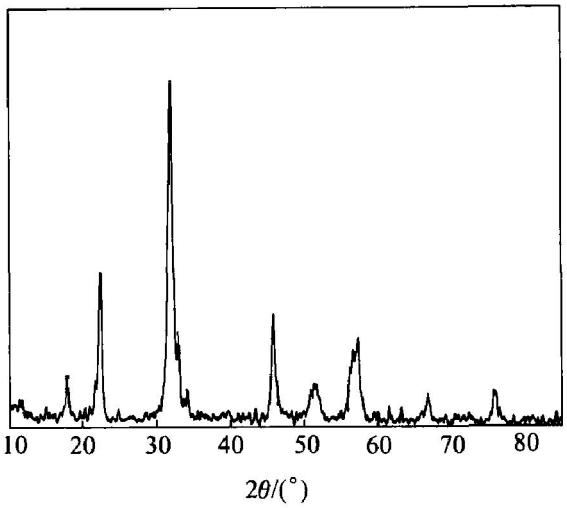

Fig. 1 XRD pattern of $CaSnO_3$ derived by wet-chemical route

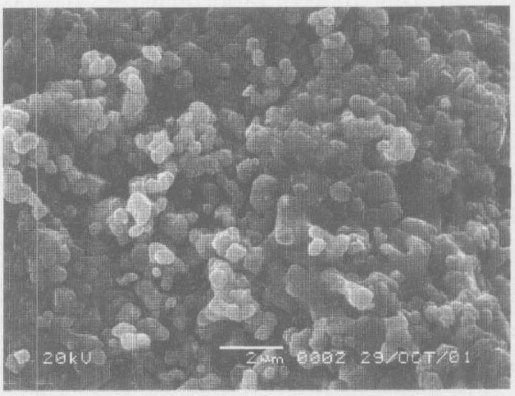

Fig. 2 SEM image of $CaSnO_3$ derived by wet-chemical route

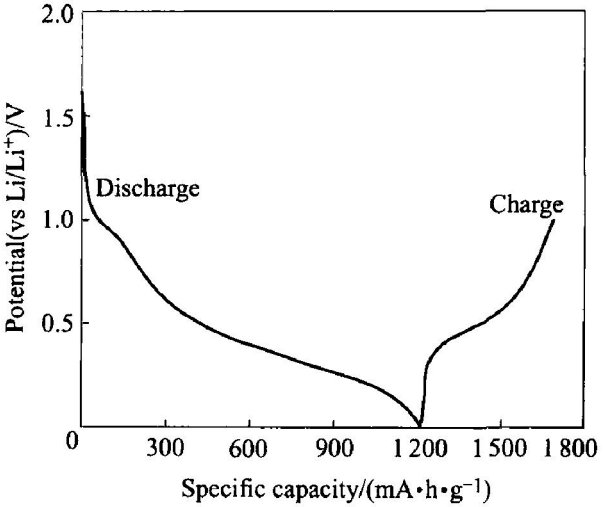

Fig. 3 First discharge and charge curves of $CaSnO_3$ anode

during first discharge is the destruction of the lattice and the formation of Sn-metal as

$$CaSnO_3 + 4Li^+ + 4e \longrightarrow CaO + 2Li_2O + Sn \quad (3)$$

This is followed by the reversible Li-Sn alloy formation as in reaction (2). The first discharge capacity (1 219 mA · h · g^{-1}) for $CaSnO_3$ electrode

corresponds to a consumption of 9.4Li, higher than the theoretical value of 8.4Li (reactions(3) and (2)). This may be due to the increased involvement of interface formation due to higher carbon content in the electrode.

The voltage profile for the first discharge for $CaSnO_3$ anode does not show extended plateau, characteristic to reaction(1) or (3), observed at about 0.9 V for SnO_2[2, 5-7] or in the voltage range 1.2 - 1.7 V observed for other Sn-oxides[2, 3, 8-10]. The profile rather resembles that observed in crystalline Sn-compounds with the inverse spinel structure, Mg_2SnO_4[9] and Zn_2SnO_4[10]. The absence of prominent plateau in the voltage range as observed for other Sn-oxides for the reduction of the crystal matrix may be due to the effect of the crystal lattice and the counter ion, Ca in $CaSnO_3$. It shows that the reduction potential for reaction(1) or (3) depends on the matrix and crystal structure in which the process takes place[8-10, 15] and a plateau potential as low as 0.15 V (vs Li) was reported in Mg_2SnO_4. MgO was not reduced to Mg metal in the latter due to large Mg—O bond strength[9]. The observed plateau at 1.0 V in $CaSnO_3$ may be due to the presence of minor amount of SnO_2 impurity not detected by XRD or characteristic of the passivating layer formation on carbon. The first charge curve shows the de-alloying reaction with less than 4.4Li(469 mA · h · g^{-1}) extraction from the compound revealing that the reaction(3) is irreversible and the reversible contribution comes from reaction(2).

The cycleability of $CaSnO_3$ anode in various potential range is shown in Fig. 4.

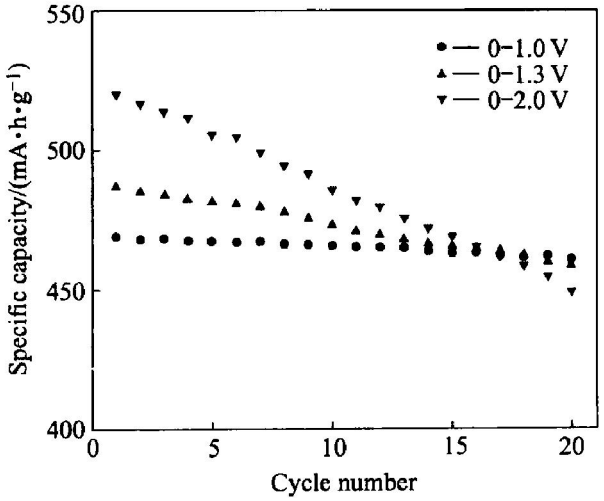

Fig. 4 Cycleability of $CaSnO_3$ anode in various potential range

When cycled in the range of 0 - 1.0 V, $CaSnO_3$ can derive a charge capacity of more than 469 mA · h · g^{-1} and the capacity loss per cycle is only 0.09%. When the upper cutoff potential range from 1.0 V to 1.3 V and 2.0 V, the charge capacity increases to 487 mA · h · g^{-1} and 520 mA · h · g^{-1}. Correspondingly, the capacity loss per cycle decreases from 0.09% to 0.30% and 0.68%, respectively. This suggests that the potential range of the cycling tests has a great influence on the cycleability of $CaSnO_3$ anode, confirming the observations made by others that the selection of voltage window of cycling for Sn-based compounds is crucial for good cycling performance[3, 6, 8]. Though the first discharge capacity is higher than the theoretical value of 8.4Li for the $CaSnO_3$, the reversible capacity is less than that expected for the de-alloying reaction (4.4Li). This may be due to the fact that the initial capacity is partly utilized for solid electrolyte interphase(SEI) formation apart from reactions(3) and (2). Further, thermodynamic and kinetic reasons can also contribute to the irreversibility. The stable and reversible capacity of 460 mA · h · g^{-1} at 0.1 *C* for $CaSnO_3$ is higher than the theoretical value for graphite (372 mA · h · g^{-1}). The attained capacity of 460 mA · h · g^{-1} and cycling stability is better than the best-performing bulk Sn-oxide based materials: ATCO (initial capacity 350 mA · h · g^{-1} and 81% retention after 40 cycles)[3] and cubic-SnP_2O_7(initial capacity, 365 mA · h · g^{-1} with 96% retention after 50 cycles)[8].

The cyclic voltammograms(CV) recorded on the cell with $CaSnO_3$ anode for the initial 20 cycles are shown in Fig. 5. Only initial 5 cycles are shown for clarity. Li-metal acts as counter and reference electrode and the scan rate is 0.1 mV/s. The first cathodic scan starts from the open circuit voltage (OCV - 2.8 V) and thereafter the voltage window is kept in the range 0 - 1.0 V. The CV profiles for the first few cycles are quite different from those reported (CV or differential capacity plots) for the ATCO or crystalline Sn-oxides[2, 3, 8]. The irreversible intense peak commonly observed for the reduction of Sn-oxide matrix (reaction(1) or (3)) is not seen in the present case. The first cathodic scan shows a very minor peak about 0.70 V and then a sharp increase in current values below 0.2 V. The subsequent anodic scan shows a peak at 0.6 V, the voltage range encountered for Li-de-alloying reaction observed in Sn-oxides. The second cathodic scan shows a broad peak starting below 0.3 V. A clear indication of peak in the cathodic scan is seen only after the third cycle at 0.16 V. On cycling, the cathodic peak moves slightly to higher voltage and the anodic one to lower voltage side and their intensity grows with cycling up to 10 cycles and remains constant up to 20 cycles indicating better reversibility of the electrode. The observed cathodic and anodic peaks can be considered to be associated with the reversible Li_xSn alloy

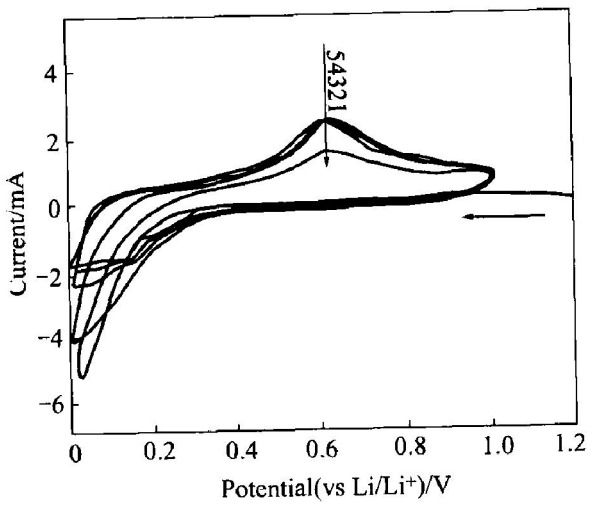

Fig. 5 Cyclic voltammograms of $CaSnO_3$ anode

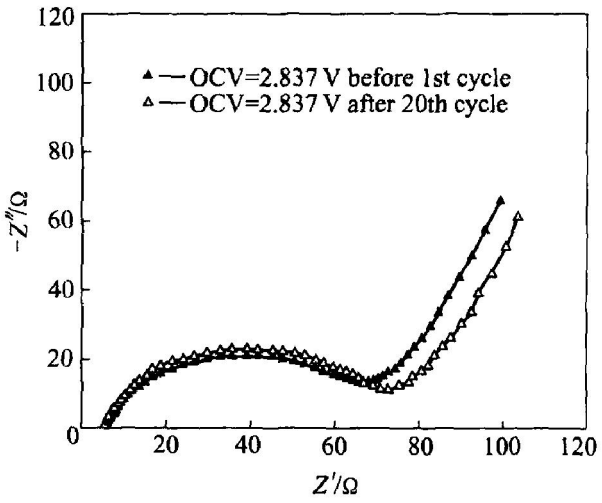

Fig. 6 AC impedance diagrams of $CaSnO_3$ anode before first and after 20th cycle

formation according to reaction (2), thereby complimenting the charge-discharge cycling data.

The absence of well-defined peak for the alloying during the initial few cathodic CV scans may be due to the formation of nano-particles of Sn in the poorly conducting (electronic) and highly amorphous matrix. In such a case Li has to diffuse through the surrounding matrix (a poor ionic as well as electronic conductor) to reach the Sn atoms, which may have a distribution of diffusion lengths and corresponding energies. With cycling, the Sn regions can segregate into bigger grains as reported by Courtney et al[2, 3] which can grow up to a critical size. The alloying and de-alloying in such regions can be considered more homogeneous, resulting in more intense CV peaks. The growth in intensity observed after the few initial cycles is in accordance with this argument. Further, the continued reduction of the compound during initial cycles, as also inferred from the cycling performance, also contribute to the redox peak intensities. Once the critical limit of segregation of Sn or full reduction of the compound is achieved, the position and intensity of the peaks are not expected to vary. Similar CV profile was also observed in SnO_2-SiO_2 nano-composite by Chen et al[16].

Fig. 6 shows the AC impedance diagrams of $CaSnO_3$ anode before the first and after the 20th cycle operated in the voltage range of 0 V to 1.0 V. A typical semicircle and an inclined line are seen in the figure. The high-frequency arc is attributed to the charge-transfer reaction at the interface of electrolyte and electrode. The inclined line corresponds to Warburg impedance related to the diffusion of lithium ion in the anode. The semicircle in the figure remains almost the same after the 20th cycle. this indicates that the charge-transfer resistance changes very little during cycling and thus the anode has good cycling behavior.

4 CONCLUSIONS

$CaSnO_3$ with perovskite structure was prepared by wet-chemical route and the electrochemical properties were studied. The wet-chemical route derives uniform nanosized crystallites of about 200 nm. The observed capacity involved in the first-discharge and the reversible capacity values during subsequent charge and discharge cycles reveal that the electrochemical process in $CaSnO_3$ is similar to other Sn-based mixed oxide materials, namely, an initial structural reduction of Sn^{4+} to Sn follows by reversible Li-Sn alloy formation. Both seem to occur at a potential below 0.3 V and is ascribed to the effect of crystal structure and counter cation (Ca). The performance of wet-chemical route derives $CaSnO_3$ with respect to the attainable capacity of 460 mA · h · g^{-1} and its retention on charge-discharge cycling is better than previously reported best-performing bulk Sn-oxides or ATCO starting materials which reveals that the perovskite structure and Ca-ion play a beneficial role.

REFERENCES

[1] Idota Y, Kubota T, Matsufuji A, et al. Tin-based amorphous oxide: a high-capacity lithium-ion-storage material [J]. Science, 1997, 276: 1395 - 1397.

[2] Courtney I A, Dahn J R. Electrochemical and in situ X-ray diffraction studies of the reaction of lithium with tin oxide composites [J]. J Electrochem Soc, 1997, 144(6): 2045 - 2052.

[3] Courtney I A, Mckinnon W R, Dahn J R. On the aggregation of tin in SnO composite glasses caused by the reversible reaction with lithium [J]. J Electrochem Soc, 1999, 146(1): 59 - 68.

[4] Winter M, Besenhard J O. Electrochemical lithiation

of tin and tin-based intermetallics and composites [J]. Electrochemica Acta, 1999, 45(1): 31-50.

[5] Liu W F, Huang X J, Wang Z X, et al. Studies of stannic oxide as an anode material for lithium-ion batteries [J]. J Electrochem Soc, 1998, 145(1): 59-62.

[6] Mohamedi M, Lee S J, Takahashi D, et al. Amorphous tin oxide films: preparation and characterization as an anode active material for lithium ion batteries [J]. Electrochimica Acta, 2001, 46(8): 1161-1168.

[7] Li N, Martin C R, Scrosati B. Nanomaterial-based Li-ion battery electrodes [J]. J Power Sources, 2001, 97-98: 240-243.

[8] Behm M, Irvine J T S. Influence of structure and composition upon performance of tin phosphate based negative electrode for lithium batteries [J]. Electrochim Acta, 2002, 47(11): 1727-1738.

[9] Connor P A, Irvine J T S. Novel tin-oxide spinel-based anodes for Li-ion batteries [J]. J Power Sources, 2001, 97-98: 223-225.

[10] Belliard F, Connor P A, Irvine J T S. Novel tin oxide-based anodes for Li-ion batteries [J]. Solid State Ionics, 2000, 135: 163-167.

[11] Azad A M, Hon N C. Characterization of $BaSnO_3$-based ceramics (Part1): synthesis, processing and microstructural development [J]. Journal of Alloys and Compounds, 1998, 270(1-2): 95-106.

[12] Mandal K D, Sastry M S, Parkash O. Preparation and characterization of calcium stannate [J]. J Mater Sci Letters, 1995, 14(17): 1412-1413.

[13] Upadhyay S, Parkash O, Kumar D. Preparation and characterization of barium stannate $BaSnO_3$ [J]. J Mater Sci Lett, 1997, 16(16): 1330-1332.

[14] HE Ze-qiang, LI Xin-hai, LIU En-hui, et al. Preparation of calcium stannate by modified wet chemical method [J]. Journal of Central South University of Technology (English Edition), 2003, 10(3): 195-197.

[15] Connor P A, Irvine J T S. Combined X-ray study of lithium(tin) cobalt oxide matrix negative electrodes for Li-ion batteries [J]. Electrochim Acta, 2002, 47(18): 2885-2892.

[16] Chen F, Shi Z, Liu M. Preparation of mesoporous SnO_2-SiO_2 composite as electrodes for lithium batteries [J]. Chem Commun, 2000(21): 2095-2096.

(Edited by LI Xiang-qun)